






Review

Applications of Artificial Intelligence in the Study and Diagnosis of Orbital Pathologies: State of the Art and Future Directions

Luca Michelutti ^{1,†} , Alessandro Tel ^{1,†} , Massimo Robiony ¹, Edoardo Agosti ² , Tamara Ius ³ ,
Giuseppe Catapano ⁴, Caterina Gagliano ^{5,6,‡}  and Marco Zeppieri ^{7,8,*} 

¹ Clinic of Maxillofacial Surgery, Head-Neck and NeuroScience Department, University Hospital of Udine, p.le S. Maria della Misericordia 15, 33100 Udine, Italy; michelutluca.uniud@gmail.com (L.M.); alessandro.tel@icloud.com (A.T.)

² Division of Neurosurgery, Department of Medical and Surgical Specialties, Radiological Sciences and Public Health, University of Brescia, Piazza Spedali Civili 1, 25123 Brescia, Italy

³ Academic Neurosurgery, Department of Neurosciences, University of Padova, 35121 Padova, Italy

⁴ Division of Neurosurgery, Department of Neurological Sciences, Ospedale del Mare, 80147 Napoli, Italy

⁵ Department of Medicine and Surgery, University of Enna “Kore”, Piazza dell’Università, 94100 Enna, Italy

⁶ Mediterranean Foundation “G.B. Morgagni”, 95125 Catania, Italy

⁷ Department of Ophthalmology, University Hospital of Udine, 33100 Udine, Italy

⁸ Department of Medicine, Surgery and Health Sciences, University of Trieste, 34127 Trieste, Italy

* Correspondence: markzeppieri@hotmail.com

† Luca Michelutti and Alessandro Tel contributed equally to this work and share the first authorship.

‡ Caterina Gagliano and Marco Zeppieri contributed equally to this work and share the last authorship.

Simple Summary

Artificial intelligence is revolutionizing the diagnosis and study of orbital diseases. Machine learning and deep learning models offer clinicians useful tools to analyze clinical data, particularly imaging data, and aid in clinical decision making. This article aims to examine how AI, particularly deep learning, can help to detect and evaluate diseases of the orbit, such as tumors, bone defects, and inflammatory diseases. Automatic segmentation and classification algorithms improve diagnostic accuracy and efficiency, while the integration of multimodal data supports clinical decisions.

Abstract

Background: Diseases of the orbit, particularly tumors, present complex diagnostic challenges due to the variability of clinical manifestations and the delicate anatomical region. Artificial intelligence could be the appropriate tool to assist the physician in clinical decision making. This review aims to investigate the potential applications of such technology for the analysis and management of orbital pathologies, investigate the advantages and limitations, and offer suggestions for future research. **Methods:** Selected studies were included for the conduct of this review by adopting the PRISMA guidelines. **Results:** AI algorithms represent an innovative tool for orbital diagnostics with potential applications in screening, surgery planning, and follow-up. Despite this, limitations and challenges persist that need to be addressed with future research. **Conclusions:** Clinical decision systems are proving to be a useful tool for the management of orbital pathology. For full integration into clinical reality, some actions are needed, including the standardization of protocols and the implementation of multicenter studies.

Keywords: artificial intelligence; orbital diseases; orbit tumors; orbital bone defects; deep learning; diagnostic imaging; clinical decision systems



Academic Editors: Arzu Tugce Guler, Ozkan Cigdem, Malik Yousef and Jeong Seop Sim

Received: 4 June 2025

Revised: 18 June 2025

Accepted: 21 June 2025

Published: 24 June 2025

Citation: Michelutti, L.; Tel, A.; Robiony, M.; Agosti, E.; Ius, T.; Catapano, G.; Gagliano, C.; Zeppieri, M. Applications of Artificial Intelligence in the Study and Diagnosis of Orbital Pathologies: State of the Art and Future Directions. *Appl. Sci.* **2025**, *15*, 7122. <https://doi.org/10.3390/app15137122>

Copyright: © 2025 by the authors. Licensee MDPI, Basel, Switzerland. This article is an open access article distributed under the terms and conditions of the Creative Commons Attribution (CC BY) license (<https://creativecommons.org/licenses/by/4.0/>).

1. Introduction: Pathologies of the Orbit and the Aim of This Study

Orbital diseases represent an extremely heterogeneous set of conditions, often complex to diagnose and treat because of the close proximity of critical structures such as the optic nerve and extraocular muscles. Often, when a lesion is identified on CT or MRI scans, the only way to understand its nature is through surgery or other invasive procedures, and, in some cases, it is not possible to clearly understand the nature of the lesion, whether benign or malignant, from clinical and radiological features alone.

With the evolution of digital technologies, artificial intelligence (AI) is gaining more and more importance and consideration as a promising tool to support clinical decision making, diagnosis, classification, and therapeutic planning of various orbital pathologies, including inflammatory, traumatic, and tumor conditions (Figure 1).

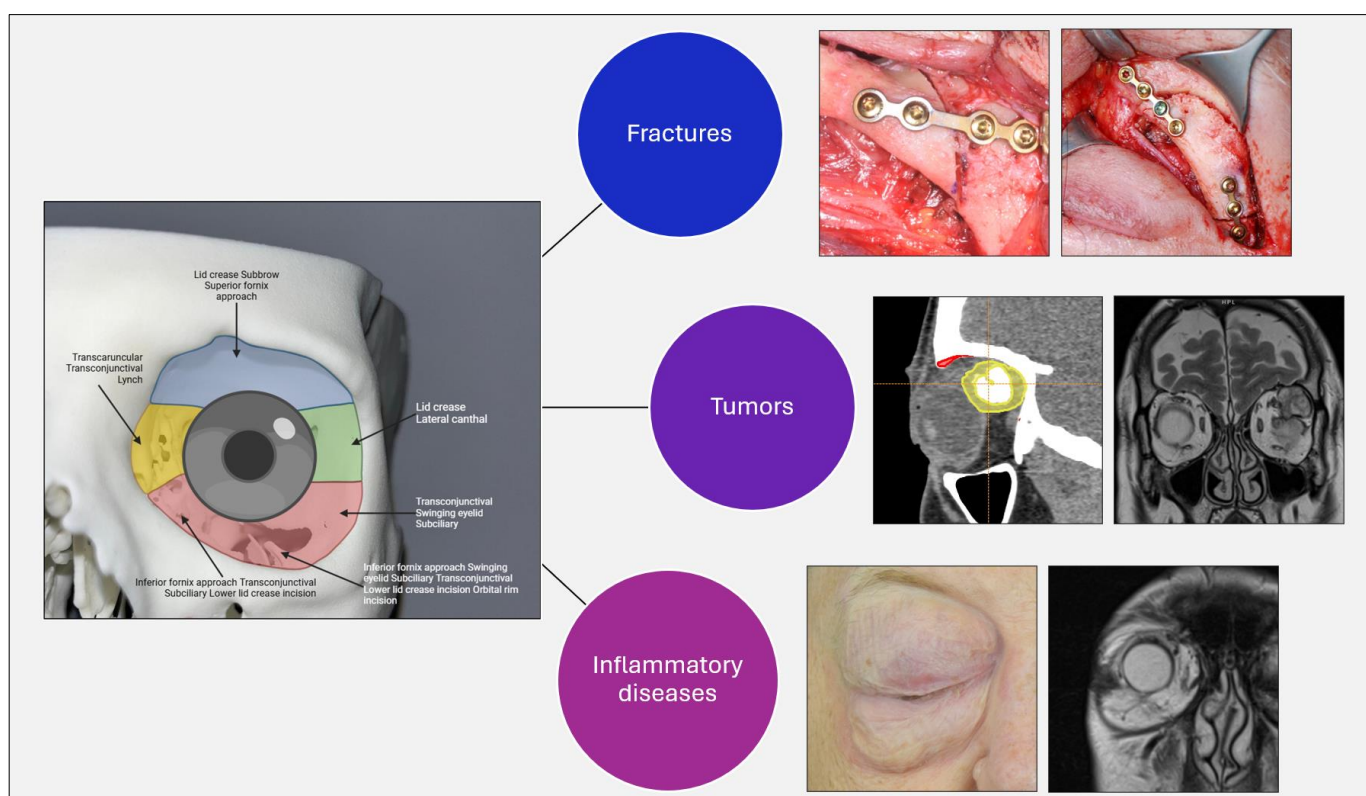


Figure 1. Graphic representation of surgical accesses and major pathologies of the orbit: fractures and bone defects, neoplastic neoformations, and inflammatory pathologies.

1.1. Space-Occupying Endorbital Lesions

Surgical pathologies of the orbit encompass a variety of conditions requiring complex and often multidisciplinary interventions. The orbit, as a confined anatomical structure surrounded by vital elements, poses significant challenges for surgeons. Numerous lesions can occur within the orbital space, either intraconal (confined within the cone formed by the extrinsic musculature), extraconal (outside of this boundary), or both. Some lesions extend beyond the orbital space to invade adjacent structures, while others originate in neighboring regions and extend into the orbit [1–3].

The causes of orbital masses are highly diverse and can be classified based on the pathological process into inflammatory, infectious, vascular, neoplastic, and congenital categories. Based on the cellular origin, orbital masses can be further classified into the following groups: primary lesions, originating directly from the orbit, including the lacrimal gland, which account for 82–87% of orbital masses; secondary lesions, extending to the orbit by contiguity from adjacent structures such as the paranasal sinuses, conjunctiva, eye,

eyelid, lacrimal sac, face, anterior and middle cranial fossae, orbital bone, nasopharynx, palate, and parotid gland, representing 9–11% of cases; and metastatic tumors, which constitute 4–8% of cases (Table 1) [2,4].

Table 1. Schematic classification of space-occupying lesions. In blue are pathologies affecting the eyeball, in green are pathologies involving the orbit, and in orange are pathologies affecting both anatomical areas.

| Category | Types of Pathologies |
|----------------------|------------------------------------------------------------------------------------------------------------------------------------------------------------------------------------------------|
| Congenital lesions | <ul style="list-style-type: none"> • Coloboma • Persistent hyperplastic primary vitreous |
| | <ul style="list-style-type: none"> • Orbital dermoid lesion • Orbital epidermoid lesion |
| Infectious lesions | <ul style="list-style-type: none"> • Ocular toxocariasis • Acute endophthalmitis |
| | <ul style="list-style-type: none"> • Orbital subperiosteal abscess • Orbital cellulitis |
| Benign tumors | <ul style="list-style-type: none"> • Lacrimal benign mixed tumor, optic pathway glioma, Coats disease, and optic nerve sheath meningioma |
| Malignant tumors | <ul style="list-style-type: none"> • Retinoblastoma • Uveal melanoma |
| | <ul style="list-style-type: none"> • Orbital Langerhans histiocytosis • Lacrimal epithelial carcinoma • Lymphoproliferative lesions • Metastases |
| Inflammatory lesions | <ul style="list-style-type: none"> • Orbital idiopathic pseudotumor, orbital sarcoidosis, thyroid ophthalmopathy, and optic neuritis |
| Vascular lesions | <ul style="list-style-type: none"> • Orbital varix • Orbital lymphatic malformation • Orbital cavernous malformations • Orbital infantile hemangioma |

The symptomatology of orbital tumors varies depending on the nature and extent of the pathology. Differential diagnosis is made based on the orbital clinical evaluation, using the mnemonic method of the seven Ps. This includes three Ps from the clinical history: pain, progression, and past medical history, as well as four Ps from the physical examination: proptosis, periocular changes, palpation, and pulsation [2,5].

The imaging techniques commonly used to evaluate the localization and extent of orbital masses are computed tomography (CT) and magnetic resonance imaging (MRI). Thin-slice, multiplanar MRI images with fat suppression and contrast enhancement allow for the delineation of orbital soft tissue lesions [2,6].

1.2. Orbital Trauma

Orbital trauma is a common cause of damage to the bony structures, soft tissues, and neurovascular components of the surrounding region. The injuries may involve only the bony orbit or be part of more complex fractures, such as those of the zygomaticomaxillary complex (ZMC) or pan-facial fractures.

1.2.1. Zygomaticomaxillary Orbital Rim Fractures

Zygomaticomaxillary orbital rim fractures, often part of larger fracture patterns such as ZMC or Le Fort fractures, affect the normal orbital contour. These fractures involve the

zygomatic bone and its connections to the maxillary and frontal bones. Physical examination may reveal palpable “step-offs,” which can guide surgical reduction. Approaches for exposure include transconjunctival, subciliary, and subtarsal incisions for the lower orbital rim, and upper blepharoplasty or lateral brow incisions for the upper rim. Minimal-invasive techniques have reduced complications like malunion, ectropion, and midface ptosis. Surgery is recommended for displaced fractures with cosmetic deformities, enophthalmos, or hypophthalmos, using open reduction internal fixation (ORIF) and orbital rim mini-plates for stabilization [7,8].

1.2.2. Orbital Floor Fracture

Orbital floor fractures, often caused by significant trauma, can lead to complications such as extraocular muscle entrapment, especially the inferior rectus muscle. This is common in pediatric patients, where greenstick fractures can result in muscle entrapment, and less frequently in adults. Entropion or restriction of eye movement in one direction suggest muscle dysfunction. Forced duction testing and CT imaging can aid in diagnosis, but are not always conclusive [7,9].

In children, an orbital fracture with symptoms like nausea and vomiting carries a high likelihood of muscle entrapment, necessitating urgent intervention. CT scans may sometimes miss entrapment or muscle injury, as local swelling can obscure clear findings [9,10].

Emergent repair is required for entrapment, particularly in cases of hypophthalmos (>2 mm) or significant fractures (>50% floor involvement). ZMC fractures may also cause posterior orbital floor buckling, requiring surgical exploration and reconstruction if there is significant displacement. Non-emergent repair is indicated for large fractures, greater than 1 cm², or those causing enophthalmos [7,9].

1.2.3. Medial Orbital Wall Fracture

Medial orbital wall fractures often occur with orbital floor fractures but can also be isolated. The medial orbital wall serves critical functions, including separating the orbital contents from the ethmoid air cells, providing a site for medial canthal tendon insertion, encasing the nasolacrimal sac, and housing the ethmoidal arteries. Small fractures can cause orbital emphysema, with air potentially leading to vascular compromise, although orbital compartment syndrome is rare. Fractures can also result in telecanthus, tear outflow obstruction, or significant hemorrhage due to ethmoidal artery injury [9,11].

Surgical repair is indicated when there is entrapment, significant defects, or >2 mm of hypophthalmos. The transcaruncular approach is preferred for its aesthetic and accessible access, though other approaches are used. Careful dissection is necessary to avoid injury to the inferior oblique muscle and nearby neurovascular structures. Plate placement over the stable posterior ledge is key to restoring orbital volume, and preformed orbital plates may be used for large defects extending to the floor. Enophthalmos is less common in isolated medial wall fractures compared to orbital floor fractures due to the lack of gravity-induced displacement into adjacent sinuses [7,9].

1.2.4. Orbital Roof Injuries

Orbital roof injuries are more common in the pediatric population due to the under-developed craniofacial skeleton, whereas, in adults, these fractures typically occur from high-impact trauma, such as motor vehicle incidents. Orbital roof fractures in adults are often associated with neurological injuries (57–90%), ocular damage (14–38%), and additional orbital and facial fractures. There is a risk of muscle entrapment, particularly involving the superior rectus, superior oblique, and trochlea, as well as exophthalmos or enophthalmos, depending on fracture displacement [9,12].

These fractures can also damage cranial contents, causing dural tears and pneumocephalus, which may increase the risk of meningitis and require neurosurgical consultation. While nondisplaced orbital roof fractures are often managed conservatively, displaced fractures may require the monitoring for intracranial pressure or surgical intervention, particularly if they lead to proptosis, hypoglobus, or exophthalmos. Surgical intervention is also indicated for diplopia, gaze restriction, or lagophthalmos caused by cranial nerve injury or muscle entrapment [9,13].

1.3. Methods and Objective of This Study

The search approach complied with PRISMA criteria. We conducted a systematic literature review utilizing the PubMed, Scopus, and Web of Science databases, encompassing the timeframe from January 2015 to April 2025. The subsequent keywords utilized were as follows: ('artificial intelligence' OR 'machine learning' OR 'deep learning') AND ('orbit' OR 'orbital pathology' OR 'orbital tumor' OR 'orbital fracture' OR 'orbital inflammation'). We incorporated authentic publications in English that reported on AI applications in orbital diseases from January 2015 to April 2025. The exclusion criteria included review papers, non-orbital applications, and studies that did not include diagnostic performance data. Supplementary filters encompassed studies involving human participants, diagnostic imaging, and the English language. Two reviewers separately performed the study selection, while a third addressed any differences.

This study aims to systematically evaluate the clinical applications of AI in the orbital setting by analyzing the type of models used, the input data employed, and the diagnostic or predictive efficacy obtained, with a focus on the validation methods and clinical outcomes reported.

2. AI for the Study of Orbital Fractures

Orbital fractures, particularly blowout fractures (BOFs), represent a challenge in maxillofacial surgery, especially because of the need for rapid and accurate diagnosis. In fact, untreated or misdiagnosed orbital fractures can lead to functional and morphologic complications, including enophthalmos, diplopia, muscle incarceration, visual deficits, and cosmetic complaints. The identification of fractures on CT images can often be complex, due to the subtlety of some bone structures or the presence of artifacts, which also results in loss of time. In addition, virtual planning of surgical reconstruction requires accurate 3D models and simulations that require time and experience. This need has opened the door to the application of artificial intelligence (AI) models in the clinical process.

2.1. Applications of AI in Orbital Fractures

Several areas of AI application in orbital fractures are reported in the literature. Regarding the diagnosis of orbital fractures, there are several deep learning (DL) models, including DenseNet, InceptionV3, and YOLOv8, which have been trained on CT images to identify the presence and location of the fracture. The study conducted by Kim et al. (2025) [14] proposed an algorithm that could distinguish whether the fracture is acute or chronic and whether it localizes to the floor, medial wall, or both, achieving 99.5% accuracy. The study conducted by Morita et al. (2024) [15] also tested object detection systems (YOLOv8 and SSD) to rapidly identify multiple facial fractures, including orbital fractures, in emergency room settings.

Another application is anatomical segmentation of the orbit, which is essential for volume calculation, preoperative simulation, and 3D model printing. Bao et al. (2023) [16] used a combination of two DL models (DenseNet-69 and U-Net) for automatic orbit segmentation and the identification of fractured regions, obtaining a superior Dice score

of 0.88 and an AUC of 0.99. In addition, the study conducted by Morita et al. (2023) [17] compared the results obtained from U-Net2D with those obtained from the study of 3D-printed models, obtaining compatible performance. In addition, the study conducted by Umapathy et al. (2020) [18] showed that the use of MRes-UNET2D enables precise segmentation of the eyeball for volumetric calculation, which is an important finding in cases of trauma.

Another interesting and innovative application is the automatic reconstruction of the orbital wall. Here, AI models are used to predict the original shape of the orbit, which is useful in cases of bilateral fractures or complex defects in which it is difficult to determine what the original anatomical shape of the orbit might be. Yu et al. (2025) [19] developed a 3D U-Net-based system capable of generating virtual reconstructions of the injured orbital wall, obtaining excellent results in terms of Hausdorff Distance at the 95th percentile (HD95) of <2.5 mm and a Structural Similarity Index (SSIM) greater than 0.98. In addition, Generative Adversarial Networks (GANs) have their place in this domain. In fact, the study conducted by Xu et al. (2025) [20] used a GAN network to generate highly symmetric and personalized surgical schedules with DSC values of >92% and Hausdorff Distance of less than 0.6 mm.

Finally, a widely used and widely accessible tool was tested as a clinical decision support, namely ChatGPT-4. The study conducted by Gernandt et al. (2024) [21] evaluated the performance of ChatGPT-4 in deciding whether an orbital fracture required surgical or conservative treatment. The model was able to correctly diagnose all fracture cases and indicate which patients required surgical treatment, while still having limitations in identifying those who would benefit from conservative treatment.

The following table (Table 2) shows the studies found in the literature regarding the application of artificial intelligence models in the diagnosis and study of orbital fractures. Information such as the models used, the input data processed by the algorithms, the evaluation method, the results, and the main benefits obtained from the individual studies are also given.

Table 2. Application of AI models for orbital fractures.

| | Objective of the Study | AI Model Used | Data Input | Results | Validation | Advantages |
|------------------------|----------------------------------------------------|-----------------------|-------------------------------------------------------------------------------------------------------------------------------------------------|------------------------------------------|--------------------------------------------------------------------|--------------------------------------------------|
| Kim et al. (2025) [14] | BOF diagnosis and classification (site and timing) | Neuro-T | A total of 233 patients, with 233 images. CT orbit in axial format, 2D images, with ROI cropped from 512 × 512 to 224 × 224 px | Accuracy 99.5%, F1 score 99.4%, AUC 0.99 | Comparison with clinical diagnosis and expert radiological reports | Complete and fast diagnosis |
| Li et al. (2020) [22] | Automatic recognition of BOF | InceptionV3 + XGBoost | A total of 94 BOF + 94 controls, with about 5640 slices. Axial orbital CT scans, 512 × 512 px slice, 3D Slicer annotations on 30 slices/patient | Accuracy 92%, AUC 0.957 | Manual annotations and comparison with experienced radiologists | AI combined with XGBoost improves classification |

Table 2. Cont.

| | Objective of the Study | AI Model Used | Data Input | Results | Validation | Advantages |
|-----------------------------|---------------------------------------|----------------------|------------------------------------------------------------------------------------------------------------------------------------------------------------------------------------|--------------------------------------------------------|--------------------------------------------------------------------------|-----------------------------------------------------|
| Bao et al. (2023) [16] | BOF segmentation | DenseNet-169 + U-Net | A total of 270 CT examinations, with 8640 slices. Axial 3D DICOM CT scans, normalized $512 \times 512 \times 32$, voxel-wise volumetric labeling | Dice 0.83, IoU 0.82, AUC 0.99 | Ground truth manual voxel-level + cross-fold validation | Precise segmentation on multi-fracture sets |
| Yu et al. (2025) [19] | Automatic reconstruction | 3D U-Net | A total of 178 simulated and real CT volumes. Three-dimensional DICOM CT, axial, $512 \times 512 \times 80$ voxels (with undeclared pitch and thickness), simulated + real dataset | HD95 < 2.5 mm, SSIM > 0.98, DSC > 0.94 | Comparison with SOTA (U-Net, DenseVoxelNet); evaluation by 3 surgeons | Reconstruction even in cases of bilateral fractures |
| Xu et al. (2025) [20] | Orbital surgical planning | GAN + SPAK | A total of 150 volumes in training and 22 real tests. Axial 3D orbital CT scans, voxel resampling at $1 \times 1 \times 1$ mm, with healthy side symmetry | DSC 92.35%, HD95 0.59 mm | Comparison with mirroring + SSM + clinical verification on 22 real cases | Fast reconstruction, 90 s |
| Morita et al. (2023) [17] | Orbit segmentation for 3D modeling | 2D U-Net | A total of 125 patients, with 3.750 slices. Two-dimensional axial orbital CT scans, 512×512 voxels, standard orientation, preprocess with CLAHE | Dice 0.86, ASSD 0.71 mm | Comparison with 3D Slicer + qualitative surgical evaluation (n = 125) | Automatically generatable STL models |
| Morita et al. (2024) [15] | Detection of orbit and face fractures | YOLOv8 + SSD | A total of 883 slices. Axial CT, images converted to PNG, bounding box annotations on 883 slices | Precision > 87%, AP > 0.89 | Train/test set manually annotated by 2 experts | Applicability in emergency/triage |
| Umapathy et al. (2020) [18] | Post-trauma bulb segmentation | MRes-UNET2D | A total of 10 training and 10 testing patients, with about 400 slices. Axial orbital CT scans, normalized grayscale images 512×512 , manual binary masks | Dice 0.95, error < 5.3% | Segmented masks from 1 neuroradiologist + 2 residents | Useful bulb volume for head injury |
| Gernandt et al. (2024) [21] | AI used for surgical decisions | ChatGPT-4 | A total of 30 vignettes with actual prompts and decisions. A total of 30 textual clinical cases + reports (without pictures), standardized prompts | Diagnosis 100%, Surgical sensitivity 57%, Kappa = 0.44 | Retrospective comparison with final surgical decisions | AI as clinical support in low-resource areas |

2.2. Advantages of AI Models for Orbital Fractures

The application of AI in the context of orbital fractures has proven beneficial, with impacts in diagnostic and surgical settings. The models studied are demonstrating per-

formance equal to or slightly better than that of humans in terms of diagnostic accuracy, both in terms of location (orbit floor vs. medial wall) and stage (acute vs. chronic) [14]. In addition, the rapid automatic and reproducible segmentation reduces the processing time from more than 20 min (for the manual one) to a few seconds. In addition, the high correlation with manual masks ensures reliability for 3D modeling and volumetric calculation [16,17]. Even in complex cases characterized by bilateral orbital fractures, AI shows that it can be a useful and valuable tool. Indeed, these models would allow the automatic reconstruction of orbital walls, enabling custom implant design and preoperative simulation [19,20]. Another aspect to be considered is the reduction in clinical burden and decision-making time, especially in emergency settings and in places without specialists or in low-resource locations, allowing a reduction in diagnosis time and the optimization of clinical workflows [15,21].

2.3. Limitations of AI Models for Orbital Fractures

However, although it seems to be a promising tool, the widespread adoption of AI in this field still presents important obstacles, both methodological and practical, such as the low generalizability of the models, since most of the included studies are based on monocentric datasets and limited samples, exposing the models to the risk of overfitting. Another limitation is the dependence on expert manual annotation. In fact, segmentations are typically trained on manual masks obtained with 3D Slicer or similar software. They also fail to always provide complex clinical decisions, as in the case of ChatGPT-4, which failed to identify patients for conservative treatment. The fact that most of these studies are retrospective also poses an obstacle, as systematic prospectives and intraoperative validation are lacking. Another consideration, last but not least, are ethical and regulatory issues, since the use of AI in diagnosis and surgery carries medico-legal implications, including the definition of liability in case of error, the lack of certification, and the need for transparency and auditability of the system.

3. AI for the Study of Orbital Tumors

Orbital tumors represent an extremely heterogeneous category of benign and malignant lesions involving the anatomical structures contained in the orbital cavity. The accurate diagnosis of these pathologies is essential to establish the correct diagnostic–therapeutic course, avoiding misdiagnosis and unnecessary or overly invasive treatment. However, the precise identification of the type of lesion, such as cavernous hemangioma, lymphoma, or squamous carcinoma, is complicated by the overlap of similar clinical signs and radiologic features. In recent years, AI has been taking an increasingly prominent role in radiologic image processing by allowing the automatic extraction of quantitative features (radiomics), the analysis of CT and MRI images, the segmentation of orbital structures, and the classification of lesions.

3.1. Applications of AI in Orbital Tumors

Several applications of AI models for the study of orbital tumors are reported in the literature. This technology is proving useful for tumor classification. In fact, one of the major areas of application is the distinction between benign and malignant tumors from CT or MRI images. For example, the study conducted by Shao et al. (2023) [23] developed a deep learning system, based on U-Net for segmentation and ResNet-34 for classification, for processing non-contrast CT scans. The system achieved an accuracy of 87% and an AUC of 0.95, demonstrating performance compatible with that of experienced clinicians. In addition, the study conducted by O'Shaughnessy et al. (2024) [24] used multiparametric

MRI scans (DWI, DCE, and IVIM) combined with a machine learning, random forest model for lesion classification as input data, obtaining an AUC of 0.90.

Another crucial application in the diagnostic pathway is differential diagnosis. In fact, the study conducted by Han et al. (2022) [25] applied a machine learning model for the analysis of non-contrast CT images to distinguish orbital cavernous hemangiomas (OCVM) from other similar lesions. Using 13 ML models and six feature selection methods, they obtained an AUC of 0.94 and an accuracy of 88%, further demonstrating that CT scans without a contrast medium, when analyzed by AI algorithms, can provide useful diagnostic data, especially in cases where a contrast medium cannot be used, such as in cases of patient allergy.

Further application is illustrated by the study conducted by Nakagawa et al. (2022) [26], where a CNN model, based on VGG16, is presented to predict orbital invasion by naso-sinus tumors, demonstrating 92% accuracy and improved performance of general radiologists from 45–49% to 94–100% when assisted by AI.

In addition to lesion classification, there are systems that can perform automatic tumor segmentation. Wang et al. (2024) [27] introduced a semi-supervised network, MSCINet, designed for orbital tumor segmentation on CT scans. The model uses a self-learning strategy with uncertainty filters and a multiscale coherence constraint, demonstrating performance aligned with supervised methods while using a limited number of annotated images.

Finally, another application found in the literature is noninvasive diagnosis on superficial clinical images. The study conducted by Sinha et al. (2024) [28] explored the use of this technology to identify ocular surface squamous neoplasia (OSSN) early and noninvasively. Clinical images of the ocular surface, combined with cytology and histological examinations, were processed by AI models to augment and improve diagnosis and guide early topical treatment, avoiding the need for invasive biopsies.

The following table (Table 3) shows the studies found in the literature regarding the application of artificial intelligence models in the diagnosis and study of orbital neoplastic lesions. Information such as the models used, the input data processed by the algorithms, the evaluation method, the results, and the main benefits obtained from the individual studies are also given.

Table 3. Applications of AI in orbital neoplastic lesions.

| | Objective of the Study | AI Model Used | Data Input | Results | Validation | Advantages |
|----------------------------------|-------------------------------------------------------------------|------------------------------------------------------------------|---------------------------------------------------------------------------------------------------------------------------------------------------------------------------------------------------------------|------------------------------------|------------------------------------------------------------------------|------------------------------------------------------------------------|
| Han et al. (2022) [25] | Distinguishing OCVM from non-OCVM | ML (SVM, SGD, RF, XGBoost) with the selection of characteristics | A total 335 total cases: axial CT images without contrast in DICOM format, typical size: 512 × 512 px, anisotropic voxels | AUC 0.9448, Accuracy 88.1% | Comparison of 13 algorithms, separate test set | Effective diagnosis without contrast, ML interpretable |
| Nakagawa et al. (2022) [26] | Assessing orbital invasion by naso-sinus tumors | CNN, VGG16 | A total 168 lesions from 148 patients, images converted to JPEG 224 × 224 px (resizing for VGG16). Coronal post-contrast CT, slice thickness of 1 mm, soft tissue kernel | Accuracy 92% | Pre/post AI comparison of 2 general radiologists; independent test set | Improved general radiologists, AI interpretable |
| O'Shaughnessy et al. (2024) [24] | Distinguishing benign and malignant tumors by multiparametric MRI | RF + SHAP | A total 113 patients, with 46 total features (18 quantitative, 26 qualitative), DICOM format images. There are 3T MRI (Philips Ingenia), sequences: DWI, IVIM, DCE, morphological, 3D, isotropic voxels ~1 mm | AUC 0.90 (full), 0.88 (lean model) | Nested cross-validation, gold standard: histology, SHAP analysis | Multi-sequence integration, AI interpretable and clinically applicable |

Table 3. Cont.

| | Objective of the Study | AI Model Used | Data Input | Results | Validation | Advantages |
|--------------------------|---------------------------------------------------|------------------|---------------------------------------------------------------------------------------------------------------------------------------------------------------------------------------------------------------|-------------------------------------------------------------|---------------------------------------------------------------------------------------------------------|-------------------------------------------------------------------------------|
| Shao et al. (2023) [23] | Segmentation and classification of orbital tumors | U-Net + ResNet34 | A total 602 images, from 64 patients, standard resolution 512×512 px; preprocessing: normalization + ROI cropping. Non-contrast axial CT, slice thickness 1–4 mm, 2D grayscale | Dice 0.89, AUC up to 0.9546 | Comparison with 3 experienced ophthalmologists; 10-fold cross-validation, interpretability via Grad-CAM | Superior performance to radiologists, segmentation + automatic classification |
| Sinha et al. (2024) [28] | Noninvasive diagnosis of OSSN | DL/ML | RGB images (ocular surface, cytology, histology), 2D digital acquisition | Sensitivity up to 80%, good agreement with histology | Comparison with histological gold standard; qualitative evaluation of performance | Noninvasive early diagnosis, useful in low-resource environments |
| Wang et al. (2024) [27] | Semi-supervised segmentation of orbital tumors | MSCINet | A total 602 images, 55 patients (Orbtum-B/M dataset); few annotated + large-scale unlabeled data. Axial CT scans, 2D slices from 3D scans; voxels $0.7 \times 0.7 \times 1.25$ mm, images 512×512 px | Dice superior to U-Net/nnUNet; high cross-scanner stability | Comparison with U-Net, FCN, nnUNet; quantitative validation on 2 public datasets | Robust segmentation even with few labels, multi-resolution scaling |

3.2. AI as a Useful Tool for Differential Diagnosis

When studying a possible orbital lesion, fundamental to the diagnostic process is the differential diagnosis. Indeed, it is important to be able to understand what the possible diagnoses of a clinically and radiologically visible lesion may be in order to understand the correct diagnostic–therapeutic course for the patient. Many cancer lesions are confused for other diseases, often inflammatory or systemic. In fact, differential diagnosis is a major challenge in clinical practice, as many lesions have overlapping clinical and radiological manifestations but require radically different therapeutic approaches. AI could offer an innovative and less invasive solution than biopsies, which are often difficult to perform, especially in frail patients.

The study conducted by Ren et al. (2024) [29] developed a radiomics system with the aim of distinguishing solitary fibrous tumors (SFTs) from orbital schwannomas, two mesenchymal tumors with similar appearance but different clinical management, achieving AUC results of 0.90 in the multicenter testing set. In addition, the study conducted by Shao et al. (2023) [30] developed a system based on LASSO + PCA + SVM, which could distinguish Ig4-related ophthalmic disease (IgG4-ROD) and orbital MALT lymphoma by obtaining an AUC of 0.82. Another study that focused on the differential diagnosis of orbital lymphoma was conducted by Tagami et al. (2024) [31], who tested a deep learning algorithm, based on XGBoost and SHAP, to distinguish it from orbital inflammatory pseudotumors, analyzing MRI scans and obtaining an AUC of 0.89. Finally, the study conducted by Zhang et al. (2025) [32] analyzed a ResNet-based convolutional neural network (CNN) model to distinguish between orbital metastases and primary orbital tumors, which is useful for rapidly guiding oncolytic staging and therapeutic treatment.

The following table (Table 4) shows studies found in the literature regarding the application of artificial intelligence models in the differential diagnosis of orbital neoplastic lesions. Information such as the models used, the input data processed by the algorithms, the method of evaluation, and the results obtained from the individual studies are also given.

Table 4. Applications of AI in the differential diagnosis of neoplastic lesions.

| | Objective of the Study | AI Model Used | Data Input | Results | Validation |
|---------------------------|--------------------------------|---------------------------|--------------------------------------------------------------------------------------|---------------------------------------|----------------------------------------------|
| Ren et al. (2024) [29] | SFT vs. schwannoma | LASSO-logistic regression | A total of 106 radiomics features. MRI T2WI + CET1WI; 3T, 1 × 1 mm resampling | AUC 0.986/0.989/0.903 | Three cohorts (train, val, multicenter test) |
| Shao et al. (2023) [30] | IgG4-ROD vs. MALT | SVM + PCA | A total of 107 features, LASSO-selected. T1WI, T2WI; 3T MRI, 3–4 mm slice, STIR, DWI | AUC up to 0.821; F1 > 0.80 | Five-fold CV on train and test setting |
| Tagami et al. (2024) [31] | LNH vs. pseudotumor | XGBoost + SHAP | MRI scans + clinic. T1/T2 + lab markers | AUC 0.887; high decision transparency | Hold-out val. + SHAP analysis |
| Zhang et al. (2025) [32] | Metastasis vs. primitive tumor | ResNet | CE-MRI dynamic sequences. Axial CE-MRI; multiparametric | AUC > 0.92; Grad-CAM interpretability | Five-fold CV + internal testing set |

3.3. Advantages of AI in the Differential Diagnosis of Neoplastic Lesions

This technology seems very promising and is proving to be a useful tool for clinicians in several respects. One of the advantages that seems to be emerging is high diagnostic accuracy, with models demonstrating high performance in both accuracy and AUC [23–25]. It is also a particularly useful support tool for less experienced radiologists. In fact, AI has improved the diagnostic performance of non-specialist radiologists [26]. The use of AI models would also enable effective analysis of CT images acquired without a contrast medium, allowing valuable information to be obtained, especially in those patients who cannot undergo these examinations, particularly because of allergies or adverse reactions to contrast. The use of AI in this field can enable precise automatic segmentations, reducing annotation time, and the reduction in inter-observer variability. In addition, AI-model-based diagnosis could be a useful tool especially in low-resource settings with few radiologists and clinical specialists, supporting peripheral centers and telemedicine.

3.4. Limitations of AI in the Differential Diagnosis of Neoplastic Lesions

Unfortunately, limitations persist and are reported by the included studies, such as low multicenter generalizability, limited transparency of deep learning models (the so-called “black-box”), dependence on image quality, and poor comparison with clinical outcomes. In fact, regarding the latter aspect, there are few studies validating AI performance with actual therapeutic outcomes or follow-up. In addition, one must consider the cost and technical expertise required to implement such technology in clinical reality, which requires appropriate hardware and software and trained personnel, and the ethical–legal and regulatory issues mentioned above.

4. AI for the Study of Inflammatory Diseases of the Orbit

Inflammatory diseases of the orbit, such as Non-Specific Orbital Inflammation (NSOI), represent complex, idiopathic, and often relapsing clinical conditions. They make up approximately 6–16% of orbital lesions, with greater prevalence in the female sex, and are characterized by variable clinical manifestations, such as dacryoadenitis, myositis, and inflammation of the lacrimal glands. Despite the well-established use of corticosteroid drugs, the recurrence rate exceeds 50 percent.

In light of the heterogeneous and multifactorial nature of NSOI, artificial intelligence (AI) is emerging as a key resource for understanding pathogenetic mechanisms, identifying biomarkers, and developing new, more precise diagnostic approaches.

4.1. Application of AI in Inflammatory Diseases of the Orbit

In the publications we have included, AI is employed in four main areas, all of which are aimed at better understanding the pathophysiology and improving the management of NSOI. First, this technology seems useful in identifying transcriptional biomarkers for differential diagnosis. In this regard, the study conducted by Wu et al. (2024) [33] developed models to identify immune biomarkers, focusing on regulatory genes such as GPR145, which is involved in macrophage activation, and constructing a diagnostic signature based on 15 genes selected by LASSO regression and SVM-RFE. The analysis showed the selective overexpression of GPR146 in NSOI, compared with healthy tissues with a higher AUC of 0.90, suggesting potential as a discriminative biomarker between inflammatory and noninflammatory conditions of the orbit.

Further exploration in this area includes the study of immune-mediated metabolism, particularly the study of glutamine and inflammation. The study conducted by Wu et al. (2024) [34] explored the role of glutamine metabolism in orbital inflammation, and the researchers used automated feature selection (LASSO and SVM-RFE) on a set of 79 glutamine-related genes and succeeded in identifying a subset of 14 genes predictive of NSOI. From this study, through the use of AI, a direct correlation between glutamine gene activity and the infiltration of immune cells, such as macrophages and lymphocytes, was shown, supporting the hypothesis of an immune-dependent metabolism as a pathophysiological role.

Another aspect is immune and orbital microenvironment analysis. In two studies, Wu et al. (2024) [33,34] applied the CIBERSORT algorithm, combined with the ESTIMATE package, to deconstruct the immune infiltration in NSOI biopsies. This analysis allowed them to computationally estimate the proportions of CD8+ T cells, M1 and M2 macrophages, dendritic cells, and natural killer cells, providing noninvasive immunologic mapping of orbital inflammation.

The study conducted by Tooley et al. (2022) [35] performed unsupervised clustering of the transcriptome of patients with orbital inflammation and succeeded in identifying three distinct molecular subtypes, including one with high inflammatory activation, one that was immunosuppressive, and that was one mixed. This study used a combination of machine learning and functional analysis (KEGG and GSVA), allowing us to hypothesize different therapeutic responses depending on the molecular phenotype.

The following table (Table 5) shows the studies found in the literature regarding the application of artificial intelligence models in the differential diagnosis of orbital neoplastic lesions. Information such as the models used, the input data processed by the algorithms, the evaluation method, and the results obtained from individual studies are also given.

Table 5. Applications of AI in Inflammatory Diseases of the Orbit.

| | Objective of the Study | AI Model Used | Data Input | Output | Validation | Advantages |
|-----------------------|----------------------------------------|---------------------------------------|---------------------------------------------------------------------------------|--------------------------------------|-------------------------------------|---------------------------------------------------------------------------|
| Wu et al. (2024) [33] | Identifying immune biomarkers for NSOI | LASSO, SVM-RFE, GSVA, GSEA, CIBERSORT | mRNA microarray (Affymetrix GPL570). Dataset GSE58331 (train), GSE105149 (test) | Signature with 15 genes hub (GPR146) | Cross-validation + external testing | Noninvasive diagnosis, high AUC (>0.90), identification of immune targets |

Table 5. Cont.

| | Objective of the Study | AI Model Used | Data Input | Output | Validation | Advantages |
|---------------------------|------------------------------------------------|------------------------------------------|--------------------------------------------------------------------------------------------------------------|---------------------------------------------------------------|------------------------------------------------------|------------------------------------------------------------------------|
| Wu et al. (2024) [34] | Analysis of glutamine metabolism genes in NSOI | LASSO, SVM-RFE, Corrplot, GO/KEGG | A total of 79 Gln-correlated genes (RNA). Dataset GSE58331 (train), GSE105149 (test), GSE63060 (validations) | A total of 14 predictive genes, immunological associations | Multilevel validation on 3 datasets | Orbital immunometabolic mapping, new pathophysiological interpretation |
| Tooley et al. (2022) [35] | Molecular clustering of NSOI | Clustering unsupervised + ML, GSVA, KEGG | RNaseq immune transcriptome. NSOI (GEO) samples, ID not specified | Three transcriptomic phenotypes with therapeutic implications | Comparison with clinical data and activated pathways | Therapeutic personalization, corticosteroid response prediction |
| Fu et al. (2021) [36] | NSOI vs. MOGAD classification | Supervised ML, logistic regression | Clinical + autoantibody serology | Autoimmune vs. inflammatory predictive model | Internal retrospective validation | Supported differential diagnosis, useful in ambiguous settings |
| Wu et al. (2024) [37] | Study of the orbital immune infiltrate | ESTIMATE, CIBERSORT, GSEA, PCA | mRNA (GPL570), orbital transcriptome. Dataset GSE105149 | Quantification of immunological population (M1, Treg, NK) | Comparison with known immune signatures | Noninvasive orbital infiltrate analysis, treatment choice guide |

4.2. Advantages of AI Models in Inflammatory Diseases of the Orbit

The use of AI in this area has several concrete and innovative advantages, including noninvasive diagnosis and the study of digital biomarkers. Indeed, RNA-based predictive models offer a noninvasive diagnostic method to potentially replace orbital biopsy. Also, the recognition of novel pathogenetic mechanisms, such as novel metabolic and immunological pathways of glutamine and inflammatory cytokines, are findings that would not have emerged with conventional statistical methods (such as t-test). Another advantage, important for future medicine, is the personalization of therapies through the identification of the patient's transcriptomic phenotype. Indeed, identifying patients with a transcriptomic phenotype is associated with a better response to corticosteroid drugs. A further advantage is the reduction in subjective bias and inter-observer error. Computational analysis of the immune infiltrate reduces the subjectivity typical of histology assessment, also improving the reproducibility of the results.

4.3. Limitations of AI Models in Inflammatory Diseases of the Orbit

In this area, despite promising and exciting results for future research, important structural limitations emerge, such as small samples and narrow datasets in the literature, which can lead to overfitting. Another obstacle is the lack of clinical and prospective validation, and no study has integrated clinical follow-up or CT/RM imaging, making it difficult to translate biomarkers into real-world decision-making tools. Another consideration that emerges is the solely transcriptomic approach. The absence of clinical phenotypes or radiological data prevents the development of multimodal models, and no model has been tested on histological specimens in hospital diagnostic settings, leading to limited applicability in clinical practice. Finally, it is noted that no economic or comparative

analyses are available on how much the use of AI improves clinical outcomes or reduces the costs of the diagnostic–therapeutic pathway.

5. Conclusions

The results of this study show that AI has shown high potential in multiple areas of orbital pathologies. In particular, deep learning models based on CT or MRI images have enabled the accurate classification of orbital fractures and tumors, benign and malignant, with AUC and accuracy values 90% higher in multiple studies. In parallel, transcriptomic analysis using machine learning models has enabled the identification of distinctive biomarkers for inflammatory diseases such as NSOI, suggesting clinical, diagnostic, and therapeutic implications with a view to increasingly personalized medicine.

While CT and MRI are the most thoroughly researched modalities, novel AI applications in other imaging fields, including ultrasonography, angiography, and carotid arteriography, have shown encouraging potential. Recent research has employed convolutional neural networks (CNNs) to examine orbital ultrasonographic data for the swift differentiation of cystic and solid masses. Likewise, AI-augmented angiography has been investigated for identifying arterial abnormalities and perfusion deficiencies in orbital tissues.

The integration of AI has shown advantages in terms of speed, standardization, and reduction in human error, particularly in diagnostic-intensive settings or in settings where specialized expertise is limited. However, the discussion also highlights the main critical issues that have emerged, including the scarcity of large, multicenter datasets, the absence of prospective studies, and the limited use of this technology in real-world clinical practice. Moreover, few studies truly integrate multimodal data (i.e., clinical, radiological, and histological), an important aspect for the full adoption of these tools in complex decision making.

The utilization of generative AI models, including GANs and diffusion-based networks, is poised to substantially improve orbital diagnostics. These models may be employed to produce synthetic imaging datasets for uncommon orbital disorders, develop resilient segmentation models, and forecast anatomical reconstructions with high accuracy for surgical planning. Their incorporation into clinical practice may expedite individualized therapy planning and enhance accessibility in data-deficient settings.

AI thus emerges as a strategic resource in the management of these diseases, with growing applications in diagnostic, predictive, and therapeutic fields. The results, to date, indicate significant potential for improving diagnostic accuracy and therapeutic personalization. However, to ensure true clinical translation of such technology, the current limitations must be overcome by promoting validated, multicenter, prospective studies, building heterogeneous datasets, and developing AI interfaces that can be integrated into clinical workflows.

Author Contributions: Conceptualization, L.M., A.T., M.R., G.C., E.A., T.I., C.G. and M.Z.; methodology, L.M., A.T., E.A., T.I., C.G. and M.Z.; validation, L.M., A.T., M.R., G.C., E.A., T.I., C.G. and M.Z.; formal analysis, L.M. and A.T.; investigation, L.M. and A.T.; resources, L.M., A.T., M.Z., T.I., E.A. and M.R.; data curation, L.M., A.T., M.R., G.C., E.A., T.I., C.G. and M.Z.; writing—original draft preparation, L.M. and A.T.; writing—review and editing, L.M. and A.T.; visualization, L.M., A.T., M.R., G.C., E.A., T.I., C.G. and M.Z.; supervision, A.T., C.G., M.Z. and M.R.; project administration, L.M., A.T., T.I., C.G. and M.Z. All authors have read and agreed to the published version of the manuscript.

Funding: This research received no external funding.

Institutional Review Board Statement: Not applicable.

Informed Consent Statement: Not applicable.

Data Availability Statement: The data are available upon request.

Conflicts of Interest: The authors declare no conflicts of interest.

References

1. Knochel, J.Q.; Osborn, A.G.; Wing, S.D. Differential Diagnosis of Lateral Orbital Masses. *J. Comput. Tomogr.* **1981**, *5*, 11–15. [[CrossRef](#)] [[PubMed](#)]
2. Mombaerts, I.; Ramberg, I.; Coupland, S.E.; Heegaard, S. Diagnosis of Orbital Mass Lesions: Clinical, Radiological, and Pathological Recommendations. *Surv. Ophthalmol.* **2019**, *64*, 741–756. [[CrossRef](#)]
3. Yan, L.; He, G.; Zhou, X.; Zheng, Y.; Zhu, Y.; Yang, J.; Zhang, M.; Zhou, Y. Contrast-Enhanced Ultrasound in the Diagnosis of Orbital Space-Occupying Lesions. *Clin. Radiol.* **2017**, *72*, 798.e1–798.e6. [[CrossRef](#)]
4. Bonavolontà, G.; Strianese, D.; Grassi, P.; Comune, C.; Tranfa, F.; Uccello, G.; Iuliano, A. An Analysis of 2,480 Space-Occupying Lesions of the Orbit From 1976 to 2011. *Ophthalmic Plast. Reconstr. Surg.* **2013**, *29*, 79–86. [[CrossRef](#)] [[PubMed](#)]
5. Nerad, J.A. *Oculoplastic Surgery: The Requisites in Ophthalmology*; Mosby: Maryland Heights, MO, USA, 2001; pp. 350–355.
6. Ro, S.-R.; Asbach, P.; Siebert, E.; Bertelmann, E.; Hamm, B.; Erb-Eigner, K. Characterization of Orbital Masses by Multiparametric MRI. *Eur. J. Radiol.* **2016**, *85*, 324–336. [[CrossRef](#)] [[PubMed](#)]
7. Lozada, K.; Cleveland, P.; Smith, J. Orbital Trauma. *Semin. Plast. Surg.* **2019**, *33*, 106–113. [[CrossRef](#)]
8. Mast, G.; Ehrenfeld, M.; Cornelius, C.-P.; Tasman, A.-J.; Litschel, R. Maxillofacial Fractures: Midface and Internal Orbit—Part II: Principles and Surgical Treatment. *Facial Plast. Surg.* **2015**, *31*, 357–367. [[CrossRef](#)]
9. Roth, F.; Koshy, J.; Goldberg, J.; Soparkar, C. Pearls of Orbital Trauma Management. *Semin. Plast. Surg.* **2010**, *24*, 398–410. [[CrossRef](#)]
10. Cohen, S.M.; Garrett, C.G. Pediatric Orbital Floor Fractures: Nausea/Vomiting as Signs of Entrapment. *Otolaryngol. Head Neck Surg.* **2003**, *129*, 43–47. [[CrossRef](#)]
11. Choi, M.; Flores, R.L. Medial Orbital Wall Fractures and the Transcaruncular Approach. *J. Craniofacial. Surg.* **2012**, *23*, 696–701. [[CrossRef](#)]
12. Haug, R.H.; Van Sickels, J.E.; Jenkins, W.S. Demographics and Treatment Options for Orbital Roof Fractures. *Oral Surg. Oral Med. Oral Pathol. Oral Radiol. Endodontology* **2002**, *93*, 238–246. [[CrossRef](#)] [[PubMed](#)]
13. Cruz, A.A.V.; Eichenberger, G.C.D. Epidemiology and Management of Orbital Fractures: *Curr. Opin. Ophthalmol.* **2004**, *15*, 416–421. [[CrossRef](#)] [[PubMed](#)]
14. Kim, S.; Koh, H.K.; Lee, H.; Shin, H.J. Deep-Learning Method for the Diagnosis and Classification of Orbital Blowout Fracture Based on Computed Tomography. *J. Oral Maxillofac. Surg.* **2025**. S0278-2391(25)00243-5. [[CrossRef](#)] [[PubMed](#)]
15. Morita, D.; Kawarazaki, A.; Soufi, M.; Otake, Y.; Sato, Y.; Numajiri, T. Automatic Detection of Midfacial Fractures in Facial Bone CT Images Using Deep Learning-Based Object Detection Models. *J. Stomatol. Oral Maxillofac. Surg.* **2024**, *125*, 101914. [[CrossRef](#)]
16. Bao, X.-L.; Zhan, X.; Wang, L.; Zhu, Q.; Fan, B.; Li, G.-Y. Automatic Identification and Segmentation of Orbital Blowout Fractures Based on Artificial Intelligence. *Transl. Vis. Sci. Technol.* **2023**, *12*, 7. [[CrossRef](#)]
17. Morita, D.; Kawarazaki, A.; Koimizu, J.; Tsujiko, S.; Soufi, M.; Otake, Y.; Sato, Y.; Numajiri, T. Automatic Orbital Segmentation Using Deep Learning-Based 2D U-Net and Accuracy Evaluation: A Retrospective Study. *J. Cranio-Maxillofac. Surg.* **2023**, *51*, 609–613. [[CrossRef](#)]
18. Umopathy, L.; Winegar, B.; MacKinnon, L.; Hill, M.; Altbach, M.I.; Miller, J.M.; Bilgin, A. Fully Automated Segmentation of Globes for Volume Quantification in CT Images of Orbits Using Deep Learning. *AJNR Am. J. Neuroradiol.* **2020**, *41*, 1061–1069. [[CrossRef](#)]
19. Yu, F.; Liu, C.; Zhong, C.; Zeng, W.; Chen, J.; Liu, W.; Guo, J.; Tang, W. 3D Deep Learning for Virtual Orbital Defect Reconstruction: A Precise and Automated Approach. *J. Craniofacial Surg.* **2025**. [[CrossRef](#)]
20. Xu, J.; Wei, Y.; Jiang, S.; Zhou, H.; Li, Y.; Chen, X. Intelligent Surgical Planning for Automatic Reconstruction of Orbital Blowout Fracture Using a Prior Adversarial Generative Network. *Med. Image Anal.* **2025**, *99*, 103332. [[CrossRef](#)]
21. Gernandt, S.; Aymon, R.; Scolozzi, P. Assessing the Accuracy of Artificial Intelligence in the Diagnosis and Management of Orbital Fractures: Is This the Future of Surgical Decision-Making? *JPRAS Open* **2024**, *42*, 275–283. [[CrossRef](#)]
22. Li, L.; Song, X.; Guo, Y.; Liu, Y.; Sun, R.; Zou, H.; Zhou, H.; Fan, X. Deep Convolutional Neural Networks for Automatic Detection of Orbital Blowout Fractures. *J. Craniofacial Surg.* **2020**, *31*, 400–403. [[CrossRef](#)] [[PubMed](#)]
23. Shao, J.; Zhu, J.; Jin, K.; Guan, X.; Jian, T.; Xue, Y.; Wang, C.; Xu, X.; Sun, F.; Si, K.; et al. End-to-End Deep-Learning-Based Diagnosis of Benign and Malignant Orbital Tumors on Computed Tomography Images. *J. Pers. Med.* **2023**, *13*, 204. [[CrossRef](#)]
24. O’Shaughnessy, E.; Senicourt, L.; Mambour, N.; Savatovsky, J.; Duron, L.; Lecler, A. Toward Precision Diagnosis: Machine Learning in Identifying Malignant Orbital Tumors With Multiparametric 3 T MRI. *Investig. Radiol.* **2024**, *59*, 737–745. [[CrossRef](#)] [[PubMed](#)]

25. Han, Q.; Du, L.; Mo, Y.; Huang, C.; Yuan, Q. Machine Learning Based Non-Enhanced CT Radiomics for the Identification of Orbital Cavernous Venous Malformations: An Innovative Tool. *J. Craniofacial Surg.* **2022**, *33*, 814–820. [[CrossRef](#)]
26. Nakagawa, J.; Fujima, N.; Hirata, K.; Tang, M.; Tsuneta, S.; Suzuki, J.; Harada, T.; Ikebe, Y.; Homma, A.; Kano, S.; et al. Utility of the Deep Learning Technique for the Diagnosis of Orbital Invasion on CT in Patients with a Nasal or Sinonasal Tumor. *Cancer Imaging* **2022**, *22*, 52. [[CrossRef](#)]
27. Wang, K.; Jin, K.; Cheng, Z.; Liu, X.; Wang, C.; Guan, X.; Xu, X.; Ye, J.; Wang, W.; Wang, S. Multi-Scale Consistent Self-Training Network for Semi-Supervised Orbital Tumor Segmentation. *Med. Phys.* **2024**, *51*, 4859–4871. [[CrossRef](#)]
28. Sinha, S.; Ramesh, P.V.; Nishant, P.; Morya, A.K.; Prasad, R. Novel Automated Non-Invasive Detection of Ocular Surface Squamous Neoplasia Using Artificial Intelligence. *World J. Methodol.* **2024**, *14*, 92267. [[CrossRef](#)]
29. Ren, J.; Yuan, Y.; Qi, M.; Tao, X. MRI-Based Radiomics Nomogram for Distinguishing Solitary Fibrous Tumor from Schwannoma in the Orbit: A Two-Center Study. *Eur. Radiol.* **2024**, *34*, 560–568. [[CrossRef](#)] [[PubMed](#)]
30. Shao, Y.; Chen, Y.; Chen, S.; Wei, R. Radiomics Analysis of T1WI and T2WI Magnetic Resonance Images to Differentiate between IgG4-Related Ophthalmic Disease and Orbital MALT Lymphoma. *BMC Ophthalmol.* **2023**, *23*, 288. [[CrossRef](#)]
31. Tagami, M.; Nishio, M.; Yoshikawa, A.; Misawa, N.; Sakai, A.; Haruna, Y.; Tomita, M.; Azumi, A.; Honda, S. Artificial Intelligence-Based Differential Diagnosis of Orbital MALT Lymphoma and IgG4 Related Ophthalmic Disease Using Hematoxylin-Eosin Images. *Graefes Arch. Clin. Exp. Ophthalmol.* **2024**, *262*, 3355–3366. [[CrossRef](#)]
32. Zhang, H.; Xu, L.; Yang, L.; Su, Z.; Kang, H.; Xie, X.; He, X.; Zhang, H.; Zhang, Q.; Cao, X.; et al. Deep Learning-Based Intratumoral and Peritumoral Features for Differentiating Ocular Adnexal Lymphoma and Idiopathic Orbital Inflammation. *Eur. Radiol.* **2025**, *35*, 1276–1289. [[CrossRef](#)] [[PubMed](#)]
33. Wu, Z.; Li, L.; Xu, T.; Hu, Y.; Peng, X.; Zhang, Z.; Yao, X.; Peng, Q. Elucidating the Multifaceted Roles of GPR146 in Non-Specific Orbital Inflammation: A Concerted Analytical Approach through the Prisms of Bioinformatics and Machine Learning. *Front. Med.* **2024**, *11*, 1309510. [[CrossRef](#)] [[PubMed](#)]
34. Wu, Z.; Li, N.; Gao, Y.; Cao, L.; Yao, X.; Peng, Q. Glutamine Metabolism-Related Genes and Immunotherapy in Nonspecific Orbital Inflammation Were Validated Using Bioinformatics and Machine Learning. *BMC Genom.* **2024**, *25*, 71. [[CrossRef](#)] [[PubMed](#)]
35. Tooley, A.A.; Tailor, P.; Tran, A.Q.; Garrity, J.A.; Eckel, L.; Link, M.J. Differentiating Intradiploic Orbital Dermoid and Epidermoid Cysts Utilizing Clinical Features and Machine Learning. *Indian J. Ophthalmol.* **2022**, *70*, 2102–2106. [[CrossRef](#)]
36. Fu, R.; Leader, J.K.; Pradeep, T.; Shi, J.; Meng, X.; Zhang, Y.; Pu, J. Automated Delineation of Orbital Abscess Depicted on CT Scan Using Deep Learning. *Med. Phys.* **2021**, *48*, 3721–3729. [[CrossRef](#)]
37. Wu, Z.; Fang, C.; Hu, Y.; Peng, X.; Zhang, Z.; Yao, X.; Peng, Q. Bioinformatic Validation and Machine Learning-Based Exploration of Purine Metabolism-Related Gene Signatures in the Context of Immunotherapeutic Strategies for Nonspecific Orbital Inflammation. *Front. Immunol.* **2024**, *15*, 1318316. [[CrossRef](#)]

Disclaimer/Publisher’s Note: The statements, opinions and data contained in all publications are solely those of the individual author(s) and contributor(s) and not of MDPI and/or the editor(s). MDPI and/or the editor(s) disclaim responsibility for any injury to people or property resulting from any ideas, methods, instructions or products referred to in the content.